

# RSC Advances



This is an *Accepted Manuscript*, which has been through the Royal Society of Chemistry peer review process and has been accepted for publication.

*Accepted Manuscripts* are published online shortly after acceptance, before technical editing, formatting and proof reading. Using this free service, authors can make their results available to the community, in citable form, before we publish the edited article. This *Accepted Manuscript* will be replaced by the edited, formatted and paginated article as soon as this is available.

You can find more information about *Accepted Manuscripts* in the [Information for Authors](#).

Please note that technical editing may introduce minor changes to the text and/or graphics, which may alter content. The journal's standard [Terms & Conditions](#) and the [Ethical guidelines](#) still apply. In no event shall the Royal Society of Chemistry be held responsible for any errors or omissions in this *Accepted Manuscript* or any consequences arising from the use of any information it contains.

## **Graphene Oxide/Vinyl Ester Resin Nanocomposite: The Effect of Graphene Oxide, Curing Kinetics, Modeling, Mechanical properties and Thermal Stability.**

Vahid Arabli <sup>1</sup>, Alireza Aghili <sup>2</sup>

<sup>1</sup> National Iranian oil company, supervision on petroleum export, research and technology directory, Tehran 15936, Iran

Postal code: 15936

Tell: +98 917 719 2205

E-mail address: [arably@yahoo.com](mailto:arably@yahoo.com), [vahid.arabli@gmail.com](mailto:vahid.arabli@gmail.com)

<sup>2</sup> Department of Polymer Engineering, Shiraz Branch, Islamic Azad University, Shiraz, Iran

Address: Sadra new town road (Km 5), Shiraz, Iran

Postal code: 71993-5

E-mail address: [alirezaaghili@yahoo.com](mailto:alirezaaghili@yahoo.com), [aghili@iaushiraz.ac.ir](mailto:aghili@iaushiraz.ac.ir)

Corresponding author: Alireza Aghili ([alirezaaghili@yahoo.com](mailto:alirezaaghili@yahoo.com), [aghili@iaushiraz.ac.ir](mailto:aghili@iaushiraz.ac.ir))

Address: Sadra new town road (Km 5), Shiraz, Iran

Postal code: 71993-5

Tell: +98 912 387 7226

Fax: +98 713 619 1638

## Abstract

The graphene oxide (GO) was synthesized and nanocomposite was achieved using different contents of the GO and Vinyl Ester Resin (VE). The suspension was sonicated in order to prevent the agglomeration. Non isothermal differential scanning calorimetry (DSC) technique was used to study the cure kinetics of neat VE and 0.3wt% GO/VE nanocomposite. Kissinger and Ozawa equations were used to determine the activation energy ( $E_a$ ). The  $E_a$  values of curing GO/VE nanocomposite showed a decrease with respect to the neat VE. It is concluded that GO has a catalytic effect in the cure reaction. The dynamic curing process was modeled to predict the degree of curing and curing rate of resin. The modeling results showed a good agreement between the experimental data and model for different heating rates (5, 10, 15 and 20 °C /min). The glass transition temperature ( $T_g$ ) was obtained by the maximum peak temperature of the loss factor curve. The  $T_g$  was increased by nearly 10 °C with the addition of 0.4 wt% GO to VE. Tensile mechanical tests were studied and the nanocomposite of 0.3wt% GO/VE showed higher elongation and tensile strength. This percent (0.3wt% GO/VE) selected for non isothermal differential scanning calorimetry (DSC) to study the cure kinetics. Scanning electron microscopy (SEM) was studied to discern the surface features and dispersion of GO. The thermal stability of the cured VE and its nanocomposite was investigated with Thermogravimetric analysis (TGA). The char yields increased with the addition of 0.3, 1.5, and 3wt% of GO to the Vinyl ester resin. The addition of GO improved the polymer flame retardancy and thermal resistance.

**Keywords:** Graphene Oxide; Vinyl Ester Resin; Mechanical Properties; Cure Kinetics; modeling.

## 1. Introduction

Vinyl ester resins are the thermoset matrixes that widely used in the composites industry. [1,2]. VE is produced by the esterification of epoxy resin with unsaturated monocarboxylic acid. They are widely used in environments that requires high corrosion and chemical resistance, water barrier properties, low moisture absorption, low shrinkage and good dimensional stability [3,4]. Generally, these resins have been used in a wide range of application as a matrix material, coating, adhesive, electronic encapsulants, marine industry, pipelines and automotive. [5-7]. The thermoset epoxy polymers can be mixed with a second phase of nanofillers such as nanospheres, nanotubes, nanoplatelets, etc. These nanocomposites improve the toughness, stiffness, strength and thermal properties [8–10]. A large number of studies have shown properties of nanocomposites reinforced with carbon nanofiber (CNF) and carbon nanotube (CNT) [11]. As a layered carbon nanomaterial, graphene with having high aspect ratios is widely used for improving mechanical, thermal and electrical properties in polymer materials. However, the high cost and poor dispersion of the CNT and CNF in the polymers, limits the range of practical application. [12–15]. The interfacial interaction between the nanomaterials and the polymer matrix plays a very important role in obtaining the quality and properties of the nanocomposite. Poor linkage between the filler and the polymer matrix will introduce defects such as voids, which consequently have a bad effect on the mechanical properties of the nanocomposite. Introducing good bonds between the nanoparticles and the polymer matrix is still a challenge for the fabrication of composite [16, 17]. Graphite flakes can be completely expanded to produce a colloidal suspension of graphene oxide (GO) sheets by simple sonication in aqueous and organic solvents in the field of homogeneous polymer nanocomposites [18].

In this study, the improved method of Hummers was used to prepare of GO. We also investigate the simple method of preparation of GO/VE composite by dispersing GO in vinyl ester resin. The effect of GO (different contents) on thermal and mechanical properties of vinyl ester resin has been studied and compared. The composite of 0.3% GO/VE was selected for DSC test to study the cure kinetics.

## 2. Experimental

### 2.1. Materials

Natural graphite flakes (100 meshes, Product Number: 332461) were supplied by Sigma-Aldrich (Saint Louis, USA). Farapol V301 epoxy vinyl ester resin (Fig.1) using Bisphenol A epoxy (42wt % Styrene content) was purchased from Farapol jam chemical industries (Hamadan, Iran). Cobalt, Dimethylaniline (DMA) and Methyl ethyl ketone peroxide (MEKP) with the trade name of Butanox LPT, Sulfuric acid ( $\text{H}_2\text{SO}_4$ ), Phosphoric acid ( $\text{H}_3\text{PO}_4$ ), Potassium permanganate ( $\text{KMnO}_4$ ), Hydrogen peroxide ( $\text{H}_2\text{O}_2$ ), Hydrochloric acid (HCl), Tetrahydrofuran (THF) solvent and other chemicals were purchased from Merck Chemicals Company.

### 2.2. Synthesis and preparation of GO

The improved method of Hummers [19] was used to prepare of GO from graphite flakes. For this reason, the mixture of concentrated  $\text{H}_2\text{SO}_4/\text{H}_3\text{PO}_4$  (360:40 ml) was added gradually with stirring to a mixture of graphite flakes/ $\text{KMnO}_4$  (3:18 g). Then, the reaction was warm up to 45 °C and mixed for 12 h. The reaction was cooled and poured onto 400 g ice with 3 ml of 30% Hydrogen peroxide ( $\text{H}_2\text{O}_2$ ). The mixture was sifted through a metal sieve (Sigma- Aldrich, 300  $\mu\text{m}$ ) and then filtered by polyester fiber. The filtrate materials were centrifuged with 4000 rpm

for 4 h, and solid product was separated. The solid product was then washed with 200 ml of water, 200 ml of 30% HCl, and 200 ml of ethanol, respectively. After each wash, the mixture was then purified following the previous protocol of sifting, filtering and centrifugation. The material remaining was coagulated with 200 ml of ether, and the mixture was filtered again. The resulting GO obtained on the filter was vacuum dried overnight at room temperature to produce the GO powder.

### 2.3. Preparation of GO/VE nanocomposite

The GO nanoparticles were dispersed in the polymeric matrix (VE) with the help of tetrahydrofuran (THF) solvent. Different weight contents of GO (0.05, 0.1, 0.4, 1.5, 3.0 wt%) was first ultrasonicated in a 50 ml of THF solvent for 1h. The homogeneous solution of GO, in THF, was then mixed with 100 g VE monomer. The mixture stirred and ultrasonicated, for 30 min. The mixture was degassed at 60 °C in a vacuum oven for 10 h to remove of solvent and all of the bubbles. Afterwards, 1.5 ml MEKP (catalyst) and 0.3% cobalt (accelerator) were added and the mixture stirred again. In this step, Some of the viscous solution was separated and used for DSC studies. The mixture was put into stainless steel mold. Then, the cured plates were allowed to precured in an oven at 80 °C for 2 h and post-cured at 120 °C for another 1 h. The cured GO/VE nanocomposite was used for SEM, TGA and mechanical tests.

### 2.4. Characterization

X-ray diffraction (XRD) was measured using a Bruker D/Max2550 V X-ray diffractor (Rigaku, Japan) with Cu K $\alpha$  radiation ( $\lambda = 1.5418 \text{ \AA}$ ) at a scan rate of  $2 \text{ min}^{-1}$  between 2–45°. Fourier transform infrared (FTIR) spectra for graphene oxide was recorded using an Excalibur 3100

FTIR (Varian, USA) between 500 and 4000  $\text{cm}^{-1}$ . TGA and DSC were studied by Mettler Toledo - TGA/DSC1 (OH, USA) under nitrogen gas flow of 22 ml/min. For starting the non isothermal DSC tests, 25 mg of the homogeneous mixture was put in the DSC sample cell at 25°C. The sample was heated by constant heating rate (5, 10, 15, and 20 °C /min). The range of temperature was from 25 to 160 °C under nitrogen gas flow of 22 ml/min. Weight loss and degradation of the GO/VE nanocomposite was investigated by the TGA under nitrogen gas flow of 22 ml/min and heating rate of 10 °C/min. For optimum properties, samples were cured at 80°C for 2 hours and post-cured at 120 °C for 1 hour before beginning TGA and SEM test. For each TGA test, amount 25 mg of the cured sample was used. Dynamic mechanical thermal analysis (DMTA) was made using a (Dynamic Mechanical Analyzer -NETZSCH, DMA 242) at 1 Hz with a constant heating rate of 3 °C/min ranging from 30 to 250 °C. The sample dimensions were 15 × 4 × 0.5 mm. The glass transition temperature ( $T_g$ ) was obtained by the maximum peak temperature of the loss factor curve. Tensile test was measured at room temperature using an Ametek Ls100plus, following the ASTM D-638. Dumbbell-shaped sample dimensions were 80 × 12.5 × 4 mm and the crosshead speed was 1.0 mm/min. SEM images were taken by TESCAN Vega TS 5136mm (Czech Republic). UP400S Powerful sonicator (Hielscher, DE) was used for dispersion of graphene oxide in GO/VE nanocomposite.

### 3. Results and discussion

#### 3.1 XRD and FT-IR evaluation

XRD patterns of graphite, graphene oxide and GO/VE nanocomposite are shown in Fig. 2. The peak at  $2\theta = 26.55$  for graphite corresponds to the diffraction of the (002) graphite plane composed to an interlayer spacing of 0.355 nm [20]. The peak at  $2\theta = 9.45$  (graphene oxide)

corresponds to the diffraction of the (002) graphite oxide plane. The interlayer spacing of the graphite oxide can be obtained according to the Bragg's law:

$$n\lambda = 2d \sin \theta$$

Where  $n$  is the diffraction series,  $\lambda$  is the X-ray wavelength, and  $d$  is the interlayer spacing of graphene oxide. The calculated value of  $d$  (0.935 nm), implying that the sample is expanded when graphite is oxidized. However, disappeared peak of graphene, indicating that the distances between the graphene layers have been greatly expanded and the layers are disordered [21].

Moreover, the FT-IR spectra of graphene oxide was taken and is shown in Fig. 3. GO Showed peak at  $3390 \text{ cm}^{-1}$  attributed to the stretching vibration of hydroxyl (OH) groups, peak at  $1720 \text{ cm}^{-1}$  attributed to the C=O stretching vibration, peak at  $1618 \text{ cm}^{-1}$  attributed to the C=C in aromatic ring, peak at  $1413 \text{ cm}^{-1}$  attributed to the -OH deformation vibration, and peak at  $1047 \text{ cm}^{-1}$  attributed to the C-O-C in epoxide [13, 22].

### 3.2. Curing Kinetics and Modeling

Non isothermal DSC was used at four heating rates (5, 10, 15, and  $20 \text{ }^\circ\text{C /min}$ ) to study kinetics of the cure reaction of VE resin with and without adding GO. The results are illustrated in Fig. 4. The exothermic peak temperature  $T_p$  for both systems containing VE and 0.3% GO +VE, shifted to lower temperatures with decreasing heating rates. The values of peak temperatures and heats of reaction are shown in Table 1. A comparison of values for both systems shows an increase in  $T_p$  for 0.3% GO+VE nanocomposite.

In the dynamic curing process, the cure rate is function of degree of cure and temperature. All kinetic models have a same basic form same as below [23]:

$$\frac{d\alpha}{dt} = k(T)f(\alpha) \quad (1)$$

In Eq. (1),  $d\alpha/dt$  is the cure reaction rate,  $k(T)$  is the rate constant and can be explained by the Arrhenius equation,  $\alpha$  is the fractional conversion at a time  $t$ ,  $f(\alpha)$  is function of  $\alpha$  and depends on the reaction mechanism. Eq. (2) shows Arrhenius equation:

$$k(T) = A e^{-(Ea/RT)} \quad (2)$$

Where  $A$  is the pre-exponential factor,  $R$  is the gas constant,  $T$  is the absolute temperature, and  $Ea$  is the activation energy. Combining Eq. (2) and (1):

$$\frac{d\alpha}{dt} = A e^{-(Ea/RT)} f(\alpha) \quad (3)$$

Eq. (4) indicates relationship between  $d\alpha/dt$  and  $d\alpha/dT$ :

$$\frac{d\alpha}{dt} = \left( \frac{dT}{dt} \right) \frac{d\alpha}{dT} \quad (4)$$

Where  $dT/dt$  is the constant heating rate  $q$ . Combining Eq. (4) into Eq. (3) and taking the logarithm:

$$\ln \left( \frac{dT}{dt} \right) = \ln A - \ln \left( \frac{d\alpha}{dT} \right) + \ln f(\alpha) + \left( - \frac{Ea}{R} \right) \frac{1}{T} \quad (5)$$

In Eq. (5), the Kissinger and Ozawa methods were used to obtain the pre-exponential factor and activation energy [24, 25].  $f(\alpha)$  depends on the mechanism of curing and may have different forms. In the autocatalytic reactions,  $f(\alpha)$  may have the following form with orders of cure reaction  $m$  and  $n$ :

$$f(\alpha) = \alpha^m (1 - \alpha)^n \quad (6)$$

Putting  $f(\alpha)$  from Eq. (6) into Eq. (5):

$$\ln\left(\frac{dT}{dt}\right) = \ln A - \ln\left(\frac{d\alpha}{dT}\right) + \ln\left[\alpha^m(1-\alpha)^n\right] + \left(-\frac{Ea}{R}\right)\left(\frac{1}{T}\right) \quad (7)$$

Following equation is the linear equation between heating rate  $dT/dt$  and the reciprocal of the peak temperature  $T_p$ :

$$\ln\left(\frac{dT}{dt}\right) = c + \left(-\frac{Ea}{R}\right)\left(\frac{1}{T_p}\right) \quad (8)$$

Where  $c$  and  $-Ea/R$  are the intercept and slope of the curve, respectively. The term of  $c$  can be explained as follows:

$$c = \ln \bar{A} - \ln\left(\frac{d\alpha}{dT}\right)_p + \ln \alpha_p^m (1 - \alpha_p)^n \quad (9)$$

Where  $\bar{A}$  is the average value of the pre exponential factors for all heating rates,  $T_p$  is the absolute temperature for exothermic peak,  $(d\alpha/dT)_p$  is the derivative of degree of cure of temperature and  $\alpha_p$  is the degree of cure at the exothermic peak. Eq. (10) indicates Kissinger equation [24], where  $q$  is the constant heating rate ( $dT/dt$ ).

$$-\ln\left(\frac{q}{T_p^2}\right) = \frac{Ea}{RT_p} - \ln\left(\frac{AR}{Ea}\right) \quad (10)$$

To determine activation energy Kissinger and Ozawa equations were used and the results are illustrated in Fig. 5 and 6, respectively. There was a very good linear relationship between heating rate and the reversal of the exothermic peak temperature  $T_p$  for Kissinger and Ozawa methods. The values of activation energy  $Ea$  were calculated from slopes of each exothermic peak and the results are given in Table 2. By comparing the activation energy for both systems of

resin (VE and 0.3% GO + VE), it can be suggested that GO as a catalyst, improved the cure reaction and decreased activation energy values. According to the Table 2, activation energies were decreased in the Ozawa method for GO/VE nanocomposite.

The isoconversional plots were obtained by using Eq. (5). The isoconversional plots indicated the details of the VE curing process. The isoconversional plots are illustrated in Fig. 7. In these figures, each curve has the same  $\alpha$ . There was a good linear relationship for all the isoconversional curves. Activation energy calculated from slope at each degree of cure for VE and 0.3% GO+VE nanocomposite. The activation energy  $Ea$  as a function of the degree of cure (conversion) is shown in Fig. 8. As shown in Fig. 8, activation energy  $Ea$  decrease by adding 0.3% of GO. The values of  $Ea$  are shown in Table 3.

In this section, the dynamic curing process was modeled to predict the degree of cure and cure rate of vinyl ester resin [26]. In the previous research [27], the curing process of resin was complicated and there were two exothermic peaks, but in this work there is only one exothermic peak. Now, we need to obtain the pre exponential factor  $A$ , activation energy  $Ea$  and orders of cure reaction ( $m$  and  $n$ ) for each reaction at the different heating rates (5, 10, 15, and 20 °C /min). The terms of pre exponential factor  $A$  and activation energy  $Ea$  achieved by the specifications of the peaks and the orders of cure reaction ( $m$  and  $n$ ) were determined by the multiple regression operations.

The rearrangement of Equation (10) gives the average pre exponential factor  $\bar{A}$ :

$$\bar{A} = \frac{e^c \left( \frac{d\alpha}{dT} \right)^p}{\alpha^{\frac{m}{p}} (1 - \alpha)^{\frac{n}{p}}} \quad (11)$$

The pre exponential factor  $A$  changes with the heating rate  $q$ . We can use a new parameter  $Ar$  ( $Ar = A/\bar{A}$ ) to find a form of the pre exponential factor  $A$  at different heating rate (5, 10, 15, and 20 °C /min).  $Ar$  is the correction factor and Apply this correction improves the fitting results.  $Ar$  changes with the heating rate  $q$ . If we replace ( $\bar{A}$ ) and ( $A/Ar$ ) in Eq. (11), yields:

$$A = Ar \frac{e^c \left( \frac{d\alpha}{dT} \right)_p}{\alpha_p^m (1 - \alpha_p)^n} \quad (12)$$

Combining Eq. (6) and (12) into Eq. (3):

$$\left( \frac{d\alpha}{dt} \right) = Ar e^c \left( \frac{d\alpha}{dT} \right)_p e^{-(Ea/RT)} \frac{\alpha_p^m (1 - \alpha_p)^n}{\alpha_p^m (1 - \alpha_p)^n} \quad (13)$$

Multiple nonlinear least squares regression method (based on the Levenberg Marquardt algorithm) was used to determine the  $Ar$ ,  $m$  and  $n$  (Eq. 13). The details of the reaction (peak) for different heating rates can be obtained from the curve fitting results. The values of the parameters of  $Ar$ ,  $m$  and  $n$  were obtained by using a multiple nonlinear regression method. The values of  $Ar$ ,  $m$  and  $n$  at different heating rates are shown in Table 4. All of the Reactions (peaks) for both systems of VE and GO/VE nanocomposite are showed the behavior of the autocatalytic reaction. The pre exponential factor at each heating rate was obtained by Using Eq. (12) and the results are listed in Table 4. The kinetic parameters for each reaction (peak) were determined and we could obtain the values of degree of cure  $\alpha$  and cure rate  $d\alpha/dt$  for each peak by solving the differential equations.

Putting Eqs. (4) and (6) into Eq. (3) and rearranging:

$$\frac{d\alpha}{dT} = \left( \frac{dT}{dt} \right)^{-1} A e^{-(E_a/RT)} a^m (1 - \alpha)^n \quad (14)$$

Equation (14) is a nonlinear differential equation. The independent variable is the absolute temperature  $T$  and the dependent variables is the degree of cure  $\alpha$ . There is no analytical solution for equations (14). The Matlab software (ode45, Runge–Kutta 4, 5 algorithm) was used to obtain the numerical solution. The values of the degree of cure  $\alpha$  were calculated at each heating rate (5, 10, 15, and 20 °C /min). The plots of the degree of cure versus the temperature for VE are shown in Fig. 9. The procedure was repeated for 0.3% GO +VE nanocomposite and the plots of the degree of cure versus the temperature are shown in Fig. 10. At all heating rates for VE and GO/VE nanocomposite, the calculated degree of cure  $\alpha$  agreed well with the experimental data. The dependence of  $d\alpha/dT$  on temperature was obtained by differentiating the degree of cure  $\alpha$  with respect to the temperature  $T$ . By Eq. (4), the cure rates  $d\alpha/dt$  for  $\alpha$  versus temperature  $T$  were calculated. The results were illustrated in Fig. 11 and 12 for VE and 0.3% GO+VE nanocomposite, respectively. As shown in Fig. 11 and 12, the calculated cure rate predicted peak in the curing process and there was a good agreement between the model and the experimental data at all heating rates.

### 3.3 Dynamic mechanical properties

The information of the storage modulus and loss factor (tan delta) of cured resin and its composites can be measured by Dynamic mechanical analysis (DMA) [28]. Fig 13a and b show the storage modulus and loss factor of neat VE and GO/VE composites. As shown in Fig. 13a, the incorporation of GO sheets implies an increase of the storage modulus in the whole temperature range. This can be well explained by the reinforcing effect of the nanofiller leading to increase of stiffness [29]. The increases of storage modulus is due to the nanofiller reinforcement and the mobility restriction of the matrix chains induced by the formed covalent

bonds between the epoxy matrix and the sheet [29,22]. The tan delta value is the ratio of the loss modulus to the storage modulus, and the peak of tan delta is often used to obtain the  $T_g$  [30]. The  $T_g$  values of GO/VE composites are listed in Table 5. As shown in Table 5 and, Fig. 13b the  $T_g$  of the GO/VE composites has shifted to a higher temperature compared with that of neat VE. The storage moduli of the composites show increase with the sheet weight loading. The wrinkled morphology of graphene oxide sheets with high specific surface area is speculated to constrain the segmental movement of matrix chains to a certain degree. Therefore, these results slightly increase the  $T_g$  value [22,31].

### 3.4. Tensile mechanical tests and fracture surface analysis of cured nanocomposites

Typical stress- strain curves of VE and its composites with different filler loadings are shown in Fig. 14a. The tensile properties are listed in Table 5. As shown in Fig. 14a and b the highest increase in tensile strength is almost 38% (from 63.03 to 87.08 MPa) at the GO loading of 0.30 wt%. Further increase in GO content impairs tensile strength slightly. Similarly, the elongation at break presents increase at the loading of 0.30 wt% and then decreases with further increasing the GO content (Fig. 14c). It can be observed that the tensile strength of the VE depends on the percent of graphene oxide. With increasing graphene oxide, vinyl ester resin becomes harder to be broken, thus the samples with a higher percent of GO shows more tensile strength. However, GO/VE nanocomposite prepared with 0.3% GO shows higher elongation and tensile strength than the GO/VE prepared with 0.4% GO. The decrease of tensile strength in higher percent of GO may be attributed to Poor linkage, weak interface, and micro bubbles formed between the resin matrix and GO. Scanning electron microscopy was used to study of different morphologies of the fracture surface. Fig. 15 shows SEM images of fracture surfaces of

cured Vinyl Ester Resin filled with different GO content. The vinyl ester resins are brittle and the graphene oxide is stiff. Therefore, addition of GO to the matrix of VE resin appearances of the fracture mechanism of crack. As shown in Fig. 15, the surface of neat VE is almost smooth. VE resin prepared with different GO shows a rough fracture surface. It can be concluded that a rough surface attributed to the polymer deformation [32].

### 3.5. Thermal Stability

The thermal stability of the cured GO/VE nanocomposite was investigated with TGA test. For more detail different contents of the GO were used. Fig. 16 indicates TGA and DTG curves of the cured VE and GO/VE nanocomposite under nitrogen flow. The weight loss rates of the nanocomposite were reduced and thermal stability was improved in the GO/VE nanocomposite. The initial decomposition temperature ( $IDT$ ), the temperature of maximum rate of weight loss ( $T_{max}$ ) and the percent of char yield ( $Ch. Y.$ ) for VE and its nanocomposites are shown in Table 6. As shown in Table 6, the char yields at 593°C increased from 6.8% to 15.2% with increasing GO loading contents to the VE. The increased thermal stability with addition of GO sheets is attributed to a higher heat capacity of sheets and a better barrier effect of GO sheets. These effects retard the volatilization of polymer decomposition products [22]. The decomposition temperature shows the cross-link density of thermoset resins. Therefore, the increase of decomposition temperature might be also interpreted by the non-stoichiometry caused by incorporation of GO in the resin matrix [33]. The increasing of char yields agrees with

the mechanism of flame retardant [34]. Thus, the addition of GO to the VE improved the polymer thermal resistance and flame retardancy.

#### 4. Conclusions

The effect of GO on the cure kinetics of VE resin in the presence of 0.3% GO was studied. To determine activation energy of cure reaction of VE, non isothermal DSC method, Ozawa and Kissinger equations were used. The  $E_a$  value of cure reaction of the GO/VE nanocomposite decreased. It is concluded that the GO acted as catalyst in the reaction of VE/GO nanocomposite. The non isothermal DSC curves of cured resin were modeled by the Matlab program. The models were agreed well with the experimental data for all heating rates (5, 10, 15, and 20 °C /min). The Dynamic mechanical analysis showed that the matrix become stiffer after adding a low content of GO sheets and the glass transition temperatures ( $T_g$ ) shifted to a higher temperature compared with neat VE. Stress-strain tests showed that the tensile strength of 0.4% GO/VE nanocomposite is less than of the 0.3% GO/VE. This decrease may be attributed to Poor linkage, weak interface, and micro bubbles formed between the resin matrix and GO. TGA tests indicated that the char yields increased with the addition of GO to the VE and improved the polymer thermal resistance and flame retardancy.

#### 5. Acknowledgements

The authors would like to thank the National Iranian Oil Company research and technology directory and Islamic Azad university of Shiraz for financial support.

## References

- [1] C. Jang, T. E. Lacy, S. R. Gwaltney, H. Toghiani, and C. U. Pittman, *Macromolecules* 2012, 45, 4876.
- [2] S-H. Liao, M.-C. Hsiao, C.-Y. Yen, C. C. M. Ma, S. J. Lee, A. Su, M. C. Tsai, M. Y. Yen, and P. L. Liu, *Journal of Power Sources*, 2010, 195, 7808.
- [3] A. Chaturvedi and A. Tiwari, *ADVANCED MATERIALS Letters*, 2013, 4, 656.
- [4] Z. Guo, T. Pereira, O. Choi, Y. Wang and H. T. Hahn, *J Mater Chem*, 2006, 16, 2800.
- [5] X. Zhang, V. Bitaraf, S. Wei, and Z. Guo, *AIChE Journal*, 2014, 60, 266.
- [6] Z. Guo, H. W. Ng, G. L. Yee, and H. T. Hahn, *J. Nanosci Nanotechnol*, 2009, 9, 3278.
- [7] E. T. Thostenson and T- W. Chou, *Carbon*, 2006, 44, 3022.
- [8] L-C. Tang, H. Zhang, S. Sprenger, L. Ye and Z. Zhang, *Composites Science and Technology*, 2012, 72, 558.
- [9] L-C. Tang, Y-J. Wan, K. Peng, Y-B. Pei, L.-B. Wu, L.-M. Chen, L. J. Shu, J-X. Jiang, and G-Q. Lai, *Composites Part A*, 2013, 45, 95.
- [10] A. M. Rafiee, J. Rafiee, Z. Wang, H. Song, Z-Z. Yu and N. Koratkar, *ACS Nano*, 2009, 3, 3884.
- [11] E. Alishahi, S. Shadlou, S. Doagou and M. R. Ayatollahi, *macromolecular Materials and Engineering*, 2013, 298, 670.
- [12] H. Kim, A. A. Abdala, C. W. Macosko, *Macromolecules*, 2010, 43, 6515.
- [13] G. Tang, Z-G. Jiang, X. Li, H-B. Zhang, S. Hong, and Z-Z. Yu, *Composites Part B: Engineering*, 2014, 67, 564.
- [14] S. Biswas, H. Fukushima, and L. T. Drzal, *Composites Part A*, 2011, 42, 371.

- [15] Z. Wang, P. Wei, Y. Qian and J Liu, *Composites Part B*, 2014, 60, 341.
- [16] Z. Guo, X. Liang, T. Pereira, R. Scaffaro, H. T. Hahn, *Composites Science and Technology*, 2007, 67, 2036.
- [17] Z. Guo, S. Wei, B. Shedd, R. Scaffaro, T. Pereira and H. T. Hahn, *J Mater Chem*, 2007, 17, 806.
- [18] Y. Zhu, S. Murali, W. Cai, X. Li, J. W. Suk, J. R. Potts, and R. S. Ruoff, *Advanced Materials*, 2010, 22, 3906.
- [19] W. S. Hummers and R. E. Offeman, *J. Am. Chem. Soc.* 1958, 80, 1339.
- [20] H-K. Jeong, Y. P. Lee, R. J. W. E. Lahaye, M-H. Park, K. H. An, I. J. Kim, C.-W. Yang, C. Y. Park, R. S. Ruoff, and Y. H. Lee, *J AM CHEM SOC*, 2008, 130, 1362.
- [21] D. A. Nguyen, Y. R. Lee, A. V. Raghu, H. M. Jeong, C. M. Shin, and B. K. Kim, *polym Int*, 2009, 58,412.
- [22] Y-J. Wan, L-C. Tang, L-X. Gong, D. Yan, Y-B. Li Li, L-B. Wu, Jn-X. Jiang, and G-Q. Lai, *Carbon*, 2014, 69, 467.
- [23] J. Gonis, G. P. Simon and W. D. Cook, *J Appl Polym Sci*, 1999, 72, 1479.
- [24] H. E. Kissinger, *Anal Chem*, 1957, 29, 1702.
- [25] T. Ozawa, *J Therm Anal Calorim*, 1970, 2, 301.
- [26] M. Hayaty, M. H. Beheshty and M. Esfandeh, *J Appl Polym Sci*, 2011, 120, 62.
- [27] V. Arabli and A. Aghili, *Advanced Composite Materials*, 2015, 24, 561.
- [28] Q. Feng, X-J. Shen, J-P. Yang, S-Y. Fu, Y-W. Mai, K. Fried, *polymer*, 2011, 52, 6037.
- [29] L-C. Tang, Y-J. Wan, D. Yan, Y.-B. Pei, L. Zhao, Y-B. Li, L-B. Wu, J-X. Jiang, G-Q. Lai, *Carbon*, 2013, 60,16.
- [30] X. Zhang, Q. He, H. Gu, S. Wei and Z.Guo, *J. Mater. Chem. C*, 2013, 1, 2886.

- [31] T. Ramanathan, A. A. Abdala, S. Stankovich, D. A. Dikin, M. Herrera-Alonso, R. D. Piner, D. H. Adamson, H. C. Schniepp, X. Chen, R. S. Ruoff, S. T. Nguyen, I. A. Aksay, R. K. Prud'Homme And L. C. Brinson, *nat nanotechnol*, 2008, 3, 327.
- [32] J. Zhu, S. Wei, J. Ryu, M. Budhathoki, G. Liang and Z. Guo, *J Mater Chem*. 2010, 20, 4937.
- [33] Q. Liu, X. Zhou, X. Fan, Ch. Zhu, X. Yao, and Zh. Liu, *Polym Plast Technol Eng*, 2012, 51, 251.
- [34] M. Gao, W. Wu and Y. Yan, *J Therm Anal Cal*, 2009, 95, 605.

### Figure captions

Fig. 1 - The reaction of diglycidyl ether of bisphenol A epoxy resin with methacrylic acid to form of vinyl ester resin.

Fig. 2 - XRD patterns of (a) graphite, graphene oxide, and Graphene (b) neat VE resin and its composites containing different content of GO.

Fig. 3 – FT-IR spectra of the graphene oxide.

Fig. 4 - Dynamic DSC curves at different heating rates for (a) VE and (b) VE + 0.3% GO.

Fig. 5 - Kissinger plots for VE and VE + 0.3% GO. The activation energies were determined by peak temperatures at heating rates of 5, 10, 15, and 20°C/min.

Fig. 6 - Ozawa plots for VE and VE + 0.3% GO. The activation energies were determined by peak temperatures at heating rates of 5, 10, 15, and 20°C/min.

Fig. 7 - Isoconversional plots for the logarithmic heating rate versus the reciprocal of the absolute temperature (T): (a) VE and (b) VE + 0.3% GO.

Fig. 8 - Activation energy ( $E_a$ ) as a function of conversion.  $E_a$  calculated by isoconversional plots.

Fig. 9 - Comparison of model and experimental data for degree of cure as a function of temperature for VE by the method based on the Kissinger and Ozawa at heating rate of 5, 10, 15 and, 20°C/min.

Fig. 10 - Comparison of model and experimental data for degree of cure as a function of temperature for VE + 0.3% GO by the method based on the Kissinger and Ozawa at heating rate of 5, 10, 15 and, 20°C/min.

Fig. 11 - Comparison of model and experimental data for Cure rate as a function of temperature for VE by the method based on the Kissinger and Ozawa at heating rate of 5, 10, 15 and, 20°C/min.

Fig. 12 - Comparison of model and experimental data for Cure rate as a function of temperature for VE + 0.3% GO by the method based on the Kissinger and Ozawa at heating rate of 5, 10, 15 and, 20°C/min.

Fig. 13 - Dynamic mechanical properties of neat VE and its composites: (a) Storage modulus and (b) Tan delta.

Fig. 14 - Tensile properties of neat VE and its composites with different filler loadings: (a) stress–strain curves, (b) tensile strength, (c) elongation at break.

Fig. 15 - SEM image of fracture surfaces of VE and GO/VE nanocomposite, (a) neat VE, (b) 0.3 wt% of GO and (c) 0.5 wt% of GO.

Fig. 16 - Thermo gravimetric analysis of cured VE and GO/VE nanocomposite, (a) TGA and (b) DTG.

Table 1 Total dynamic heat of cure reaction and dependence of the peak properties at different heating rates (5, 10, 15, and 20 °C /min).

Sample	VE				VE + 0.3% GO			
	5	10	15	20	5	10	15	20
Heat of reaction(J/g)	65.06	65.13	61.84	74.51	71.18	66.12	63.98	78.28
$T_p$ (K)	350.15	363.65	372.55	378.67	351.15	366.45	374.25	383.15
$(d\alpha/dT)$ (1/K)	0.00283	0.00275	0.00268	0.00264	0.00285	0.00273	0.00267	0.00261
$\ln(q/T^2p)$	-10.11	-9.489	-9.133	-8.774	-10.11	-9.505	-9.14	-8.901

Table 2  $E_a$  values determined by Kissinger and Ozawa method.

	VE	VE + 0.3% GO
$E_a$ (kJ/mol) <sup>a</sup>	56.6	43.6
$E_a$ (kJ/mol) <sup>b</sup>	59.8	49

<sup>a</sup> Kissinger method, <sup>b</sup> Ozawa method

Table 3 Ea values determined by isoconversional plots with different  $\alpha$  Values.

	$\alpha$										
	5%	10%	20%	30%	40%	50%	60%	70%	80%	90%	95%
$E_a$ (kJ/mol) <sup>a</sup>	61.00	59.81	57.82	56.36	55.34	54.53	53.90	53.16	52.22	50.54	49.07
$E_a$ (kJ/mol) <sup>b</sup>	38.94	38.67	38.65	38.97	39.35	39.64	39.87	39.92	39.74	39.28	38.91

<sup>a</sup> (VE), <sup>b</sup> (VE + 0.3% GO)

Table 4 Dynamic Kinetic Parameters obtained by a Multiple Nonlinear Least-Squares Regression.

	Heating rate(°C/min)	Ar	ln(A)	m	n
VE	5	0.12583	13.87911858	0.53746	0.9475
	10	0.14729	13.92202914	0.50535	1.0254
	15	0.14210	13.77594843	0.48115	0.9262
	20	0.13959	13.85013758	0.50958	1.0521
VE + 0.3% GO	5	0.12213	9.871135344	0.44666	0.8000
	10	0.12652	10.02502643	0.55969	0.8610
	15	0.14395	10.08545156	0.53159	0.9103
	20	0.14151	10.15694283	0.62305	1.0042

Table 5 Mechanical and thermal properties of neat VE and its composites with different filler loadings.

Sample	Tensile Strength (MPa)	Elongation at Break (%)	T <sub>g</sub> (°C)
Neat VE	63.03 ± 5.03	3.99 ± 0.44	159.0
VE + 0.05% GO	68.15 ± 4.88	4.18 ± 0.64	161.1
VE + 0.1% GO	80.30 ± 5.14	5.46 ± 0.69	163.5
VE + 0.3% GO	87.08 ± 5.33	5.91 ± 0.39	166.2
VE + 0.4% GO	84.10 ± 5.10	5.72 ± 0.55	169.1

Table 6 Thermal degradation data of the cured samples.

Sample	IDT(°C) <sup>a</sup>	T(°C) <sup>b</sup>	T <sub>max</sub> (°C) <sup>c</sup>	Chr. Y(%) <sup>d</sup>
Neat VE	338	377.38	419.41	6.7
VE + 0.3% GO	339	378.45	419.55	7.1
VE + 1.5% GO	339	381.51	419.10	8.3
VE + 3.0% GO	340	380.01	420.51	15.2

<sup>a</sup> Initial Decomposition Temperature, <sup>b</sup> Temperature for 10% of weight loss, <sup>c</sup> Temperature of maximum weight loss, <sup>d</sup> Char

Yield at 593 °C

Figures:

**Graphene Oxide/Vinyl Ester Resin Nanocomposite: The Effect of Graphene Oxide, Curing Kinetics, Modeling, Mechanical properties and Thermal Stability.**

Vahid Arabli, Alireza Aghili

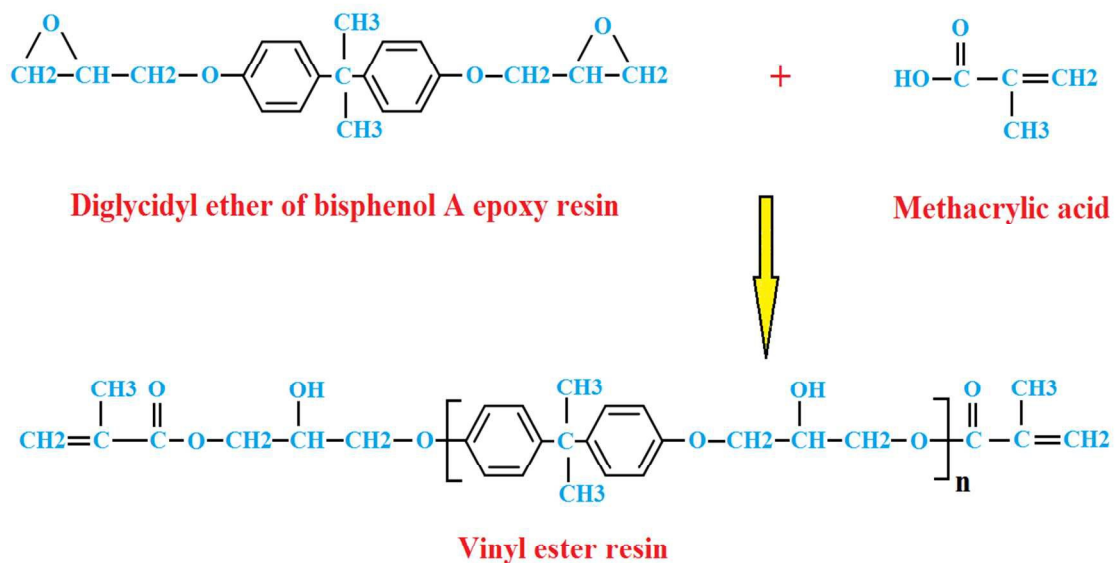


Figure 1

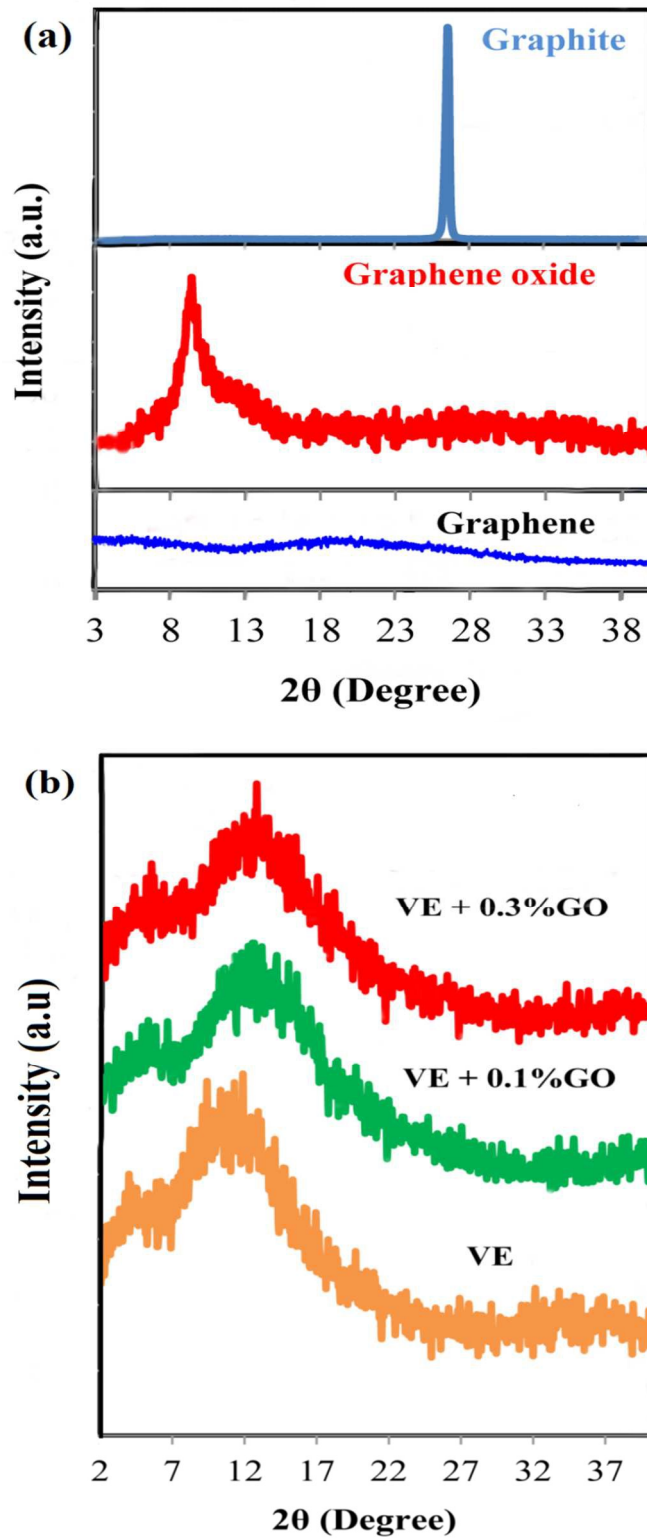


Figure 2

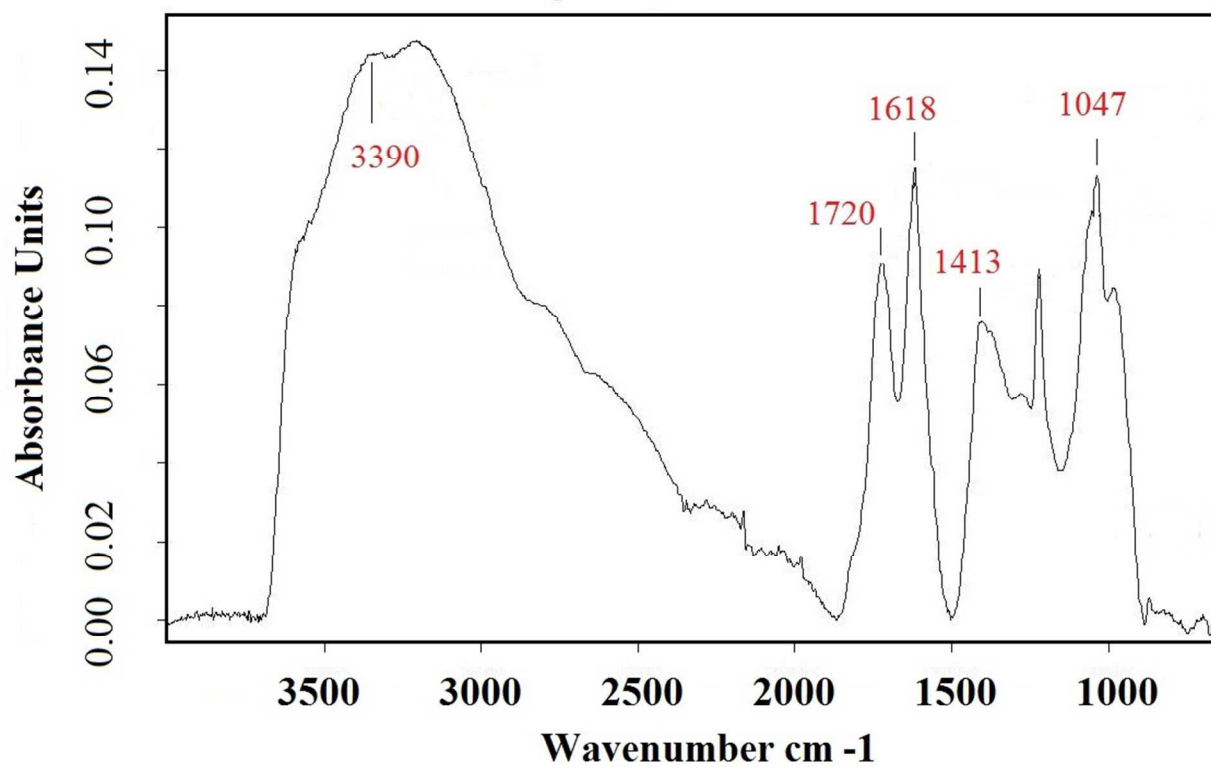


Figure 3

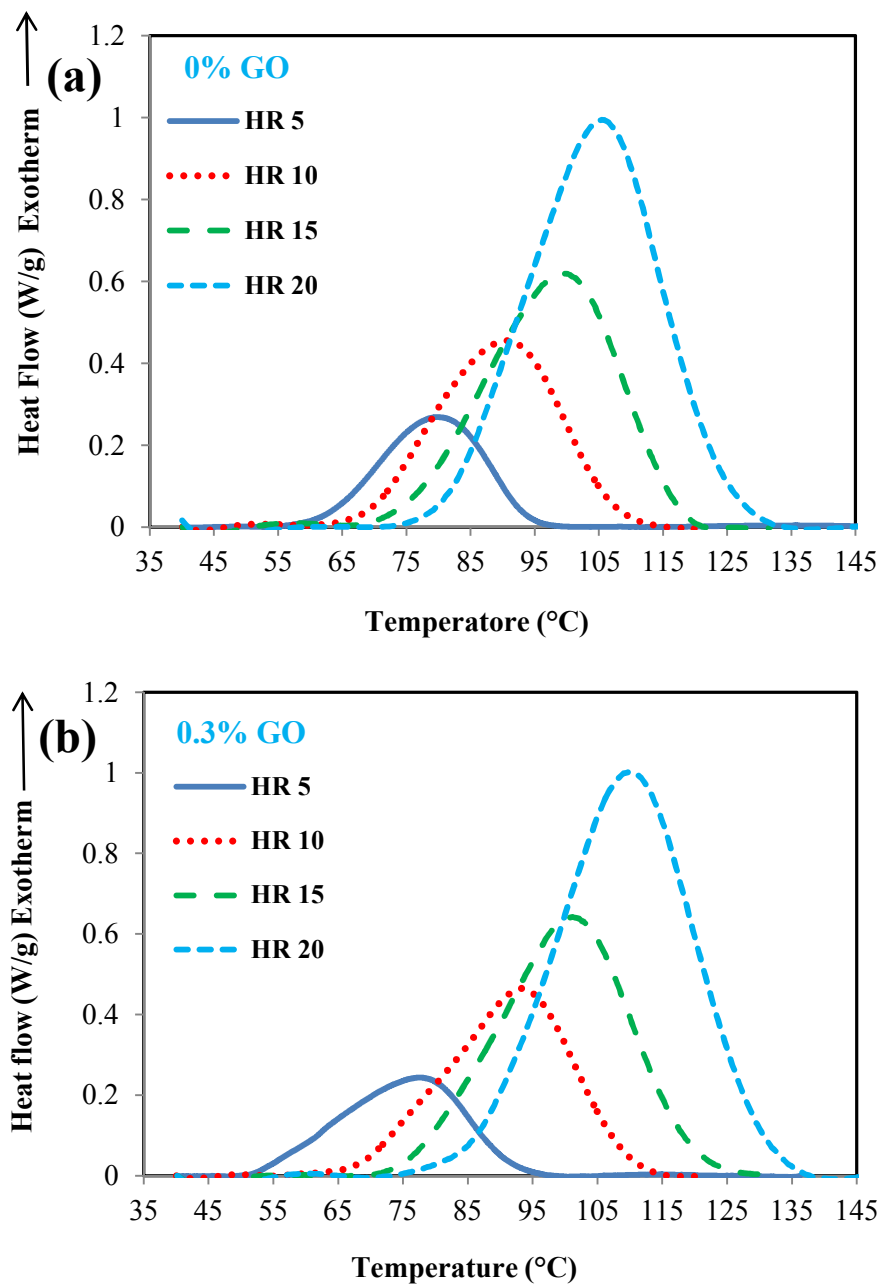


Figure 4

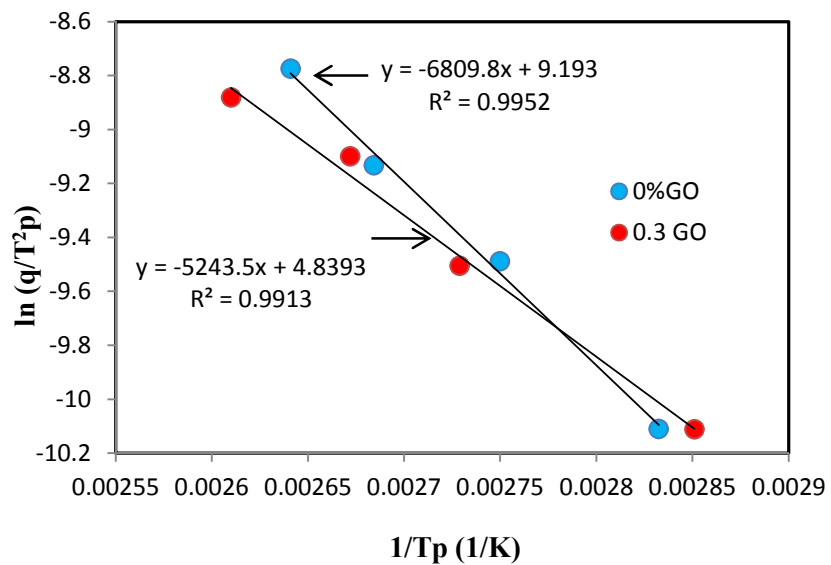


Figure 5

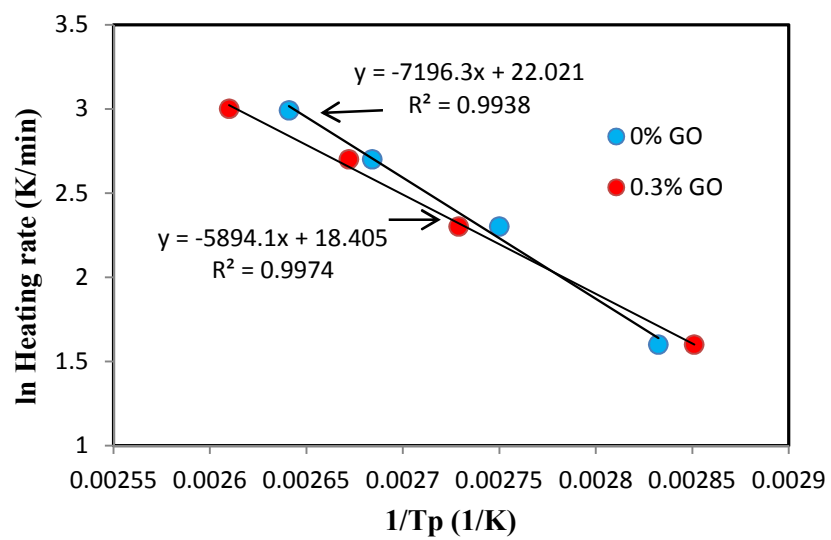


Figure 6

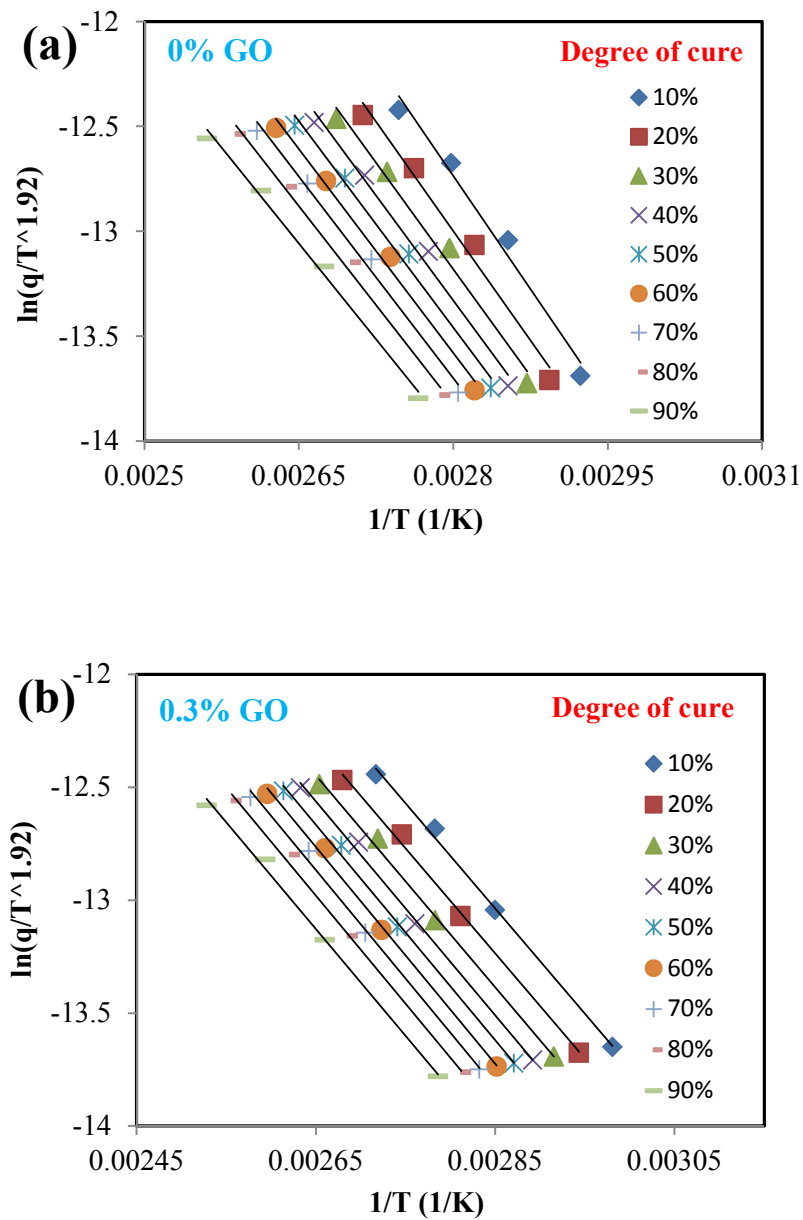


Figure 7

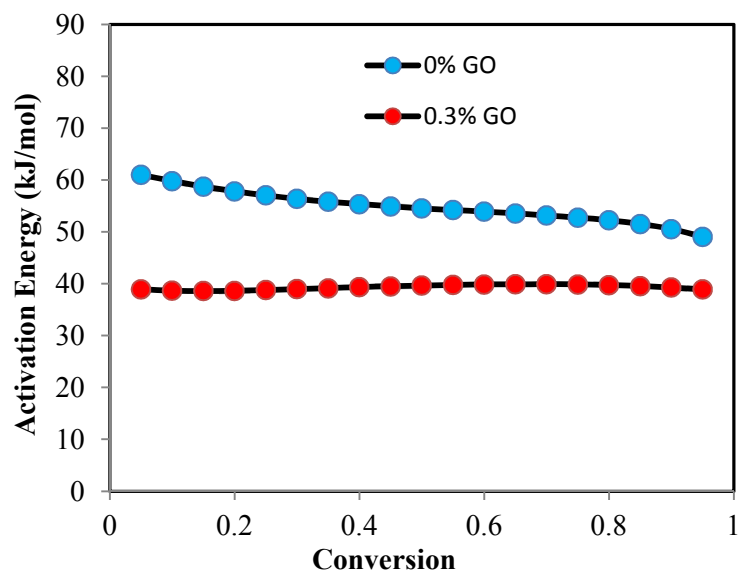


Figure 8

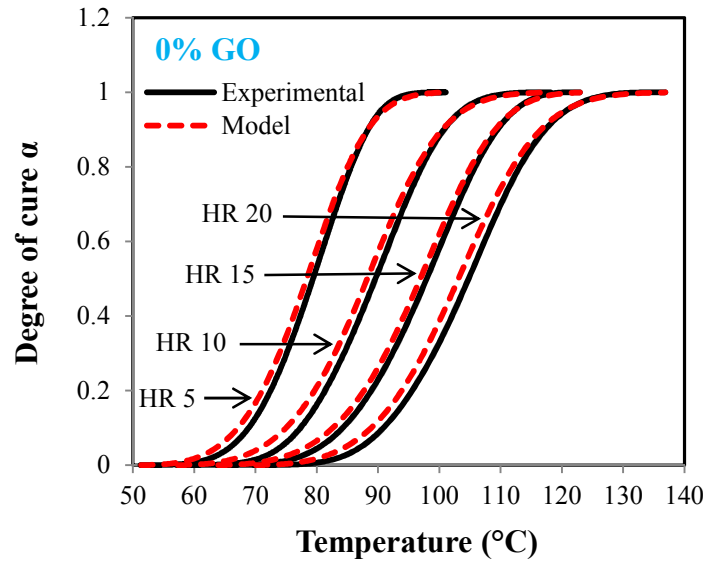


Figure 9

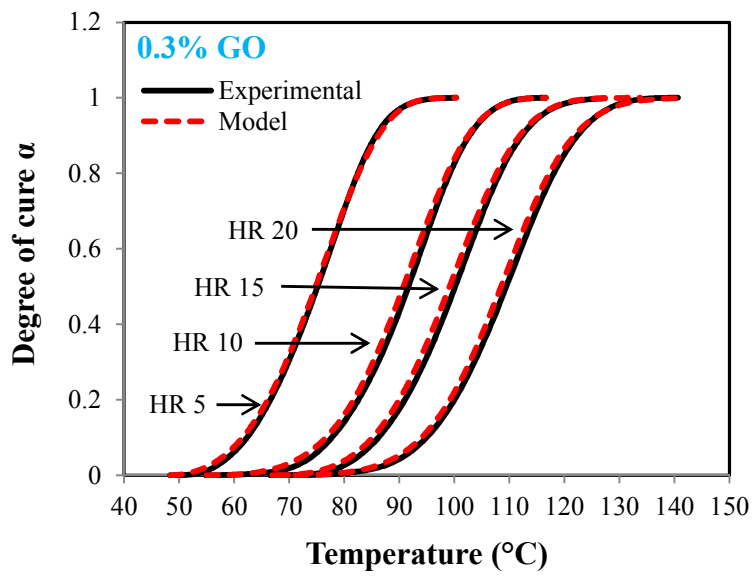


Figure 10

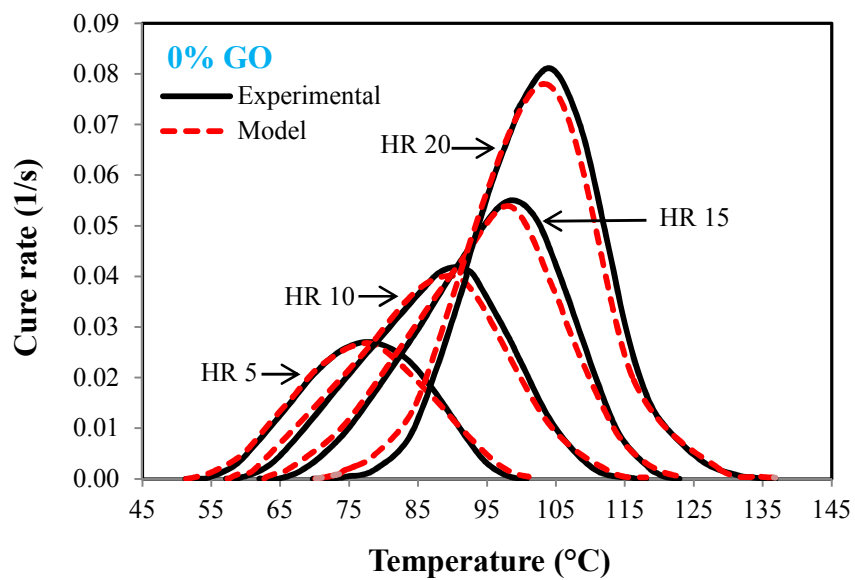


Figure 11

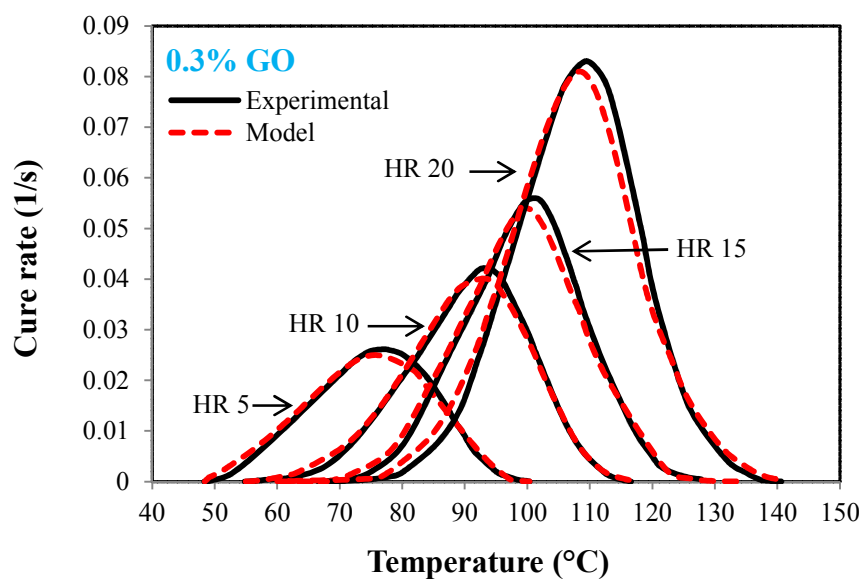


Figure 12

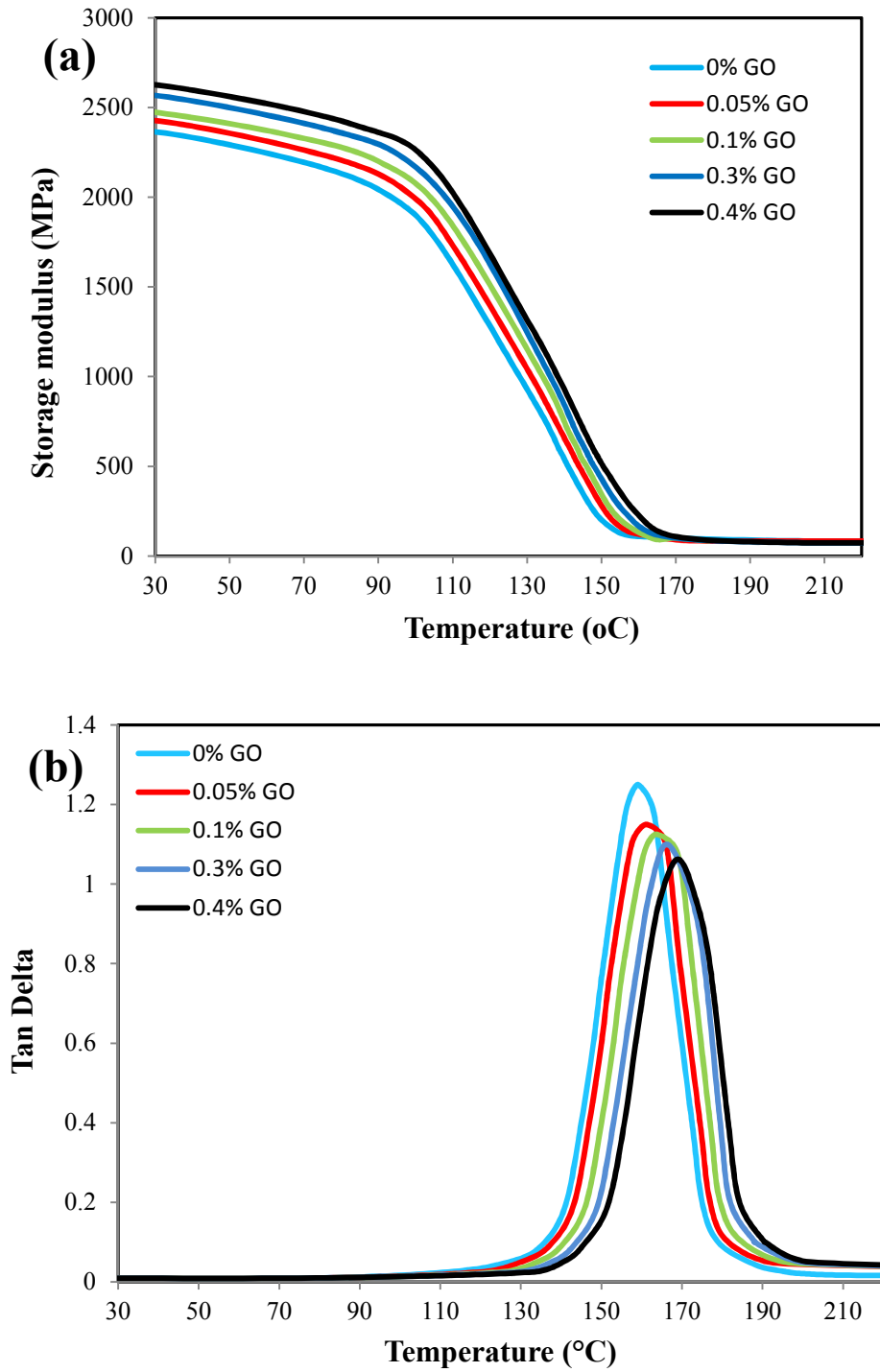


Figure 13

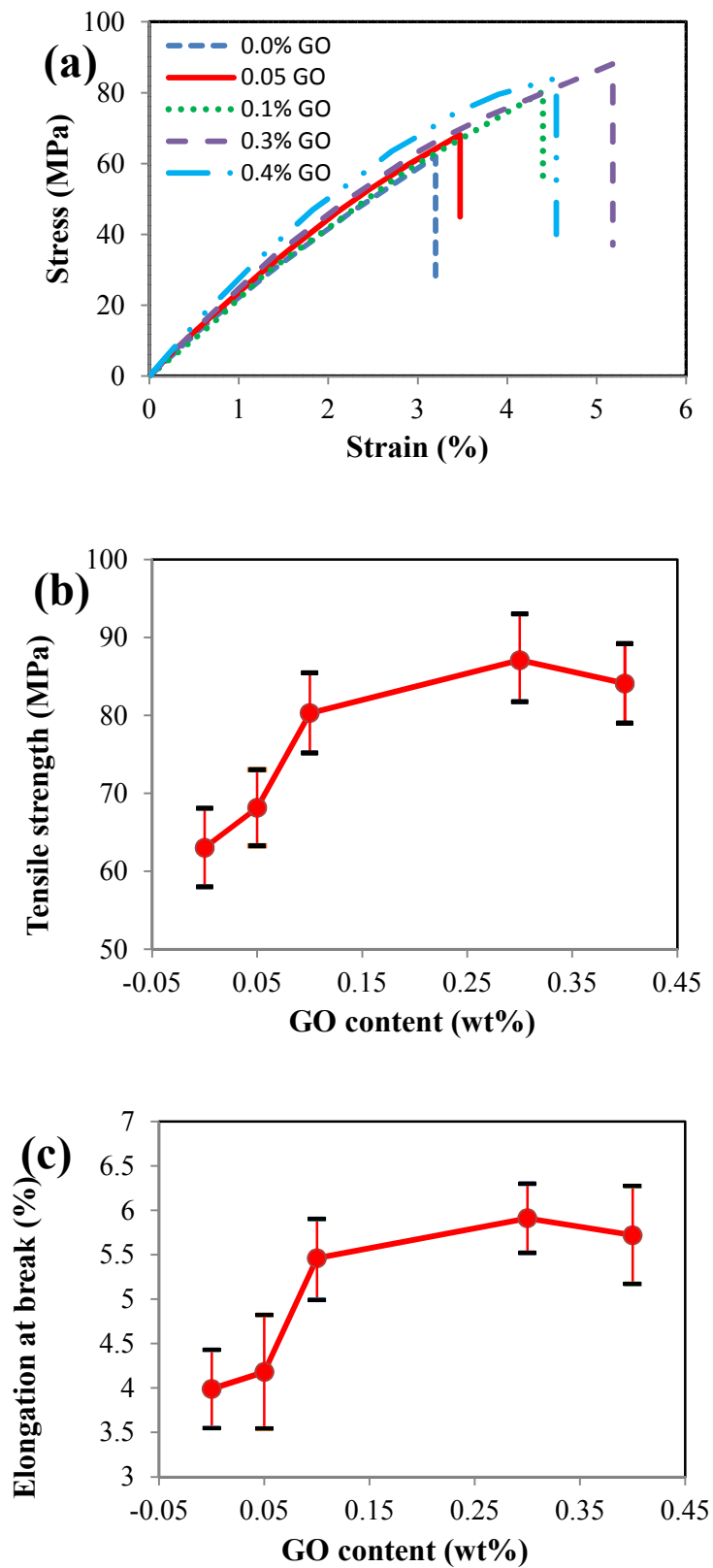
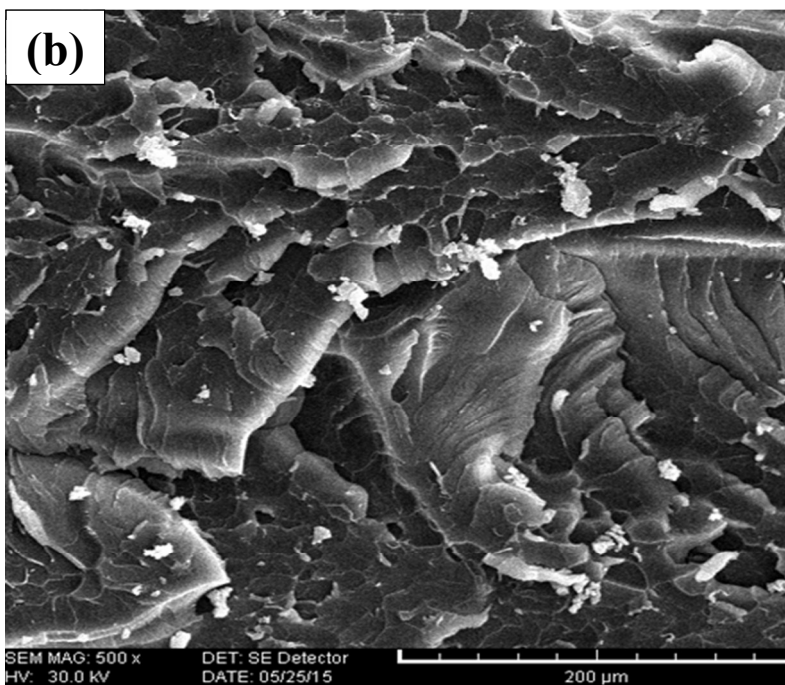
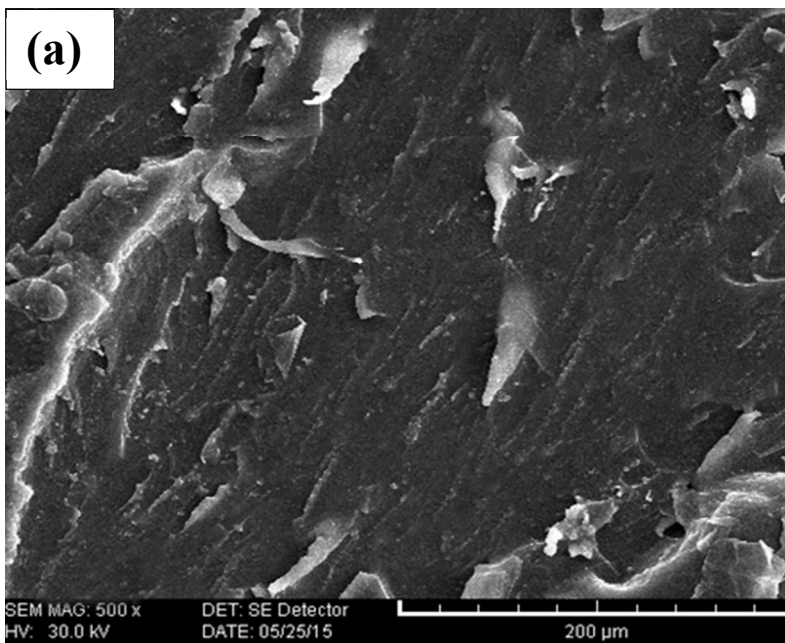


Figure 14



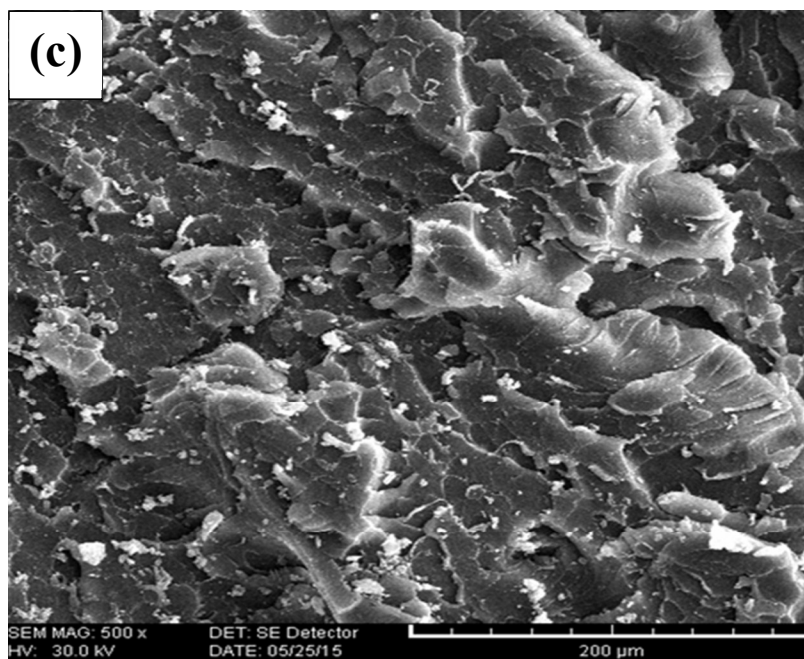


Figure 15

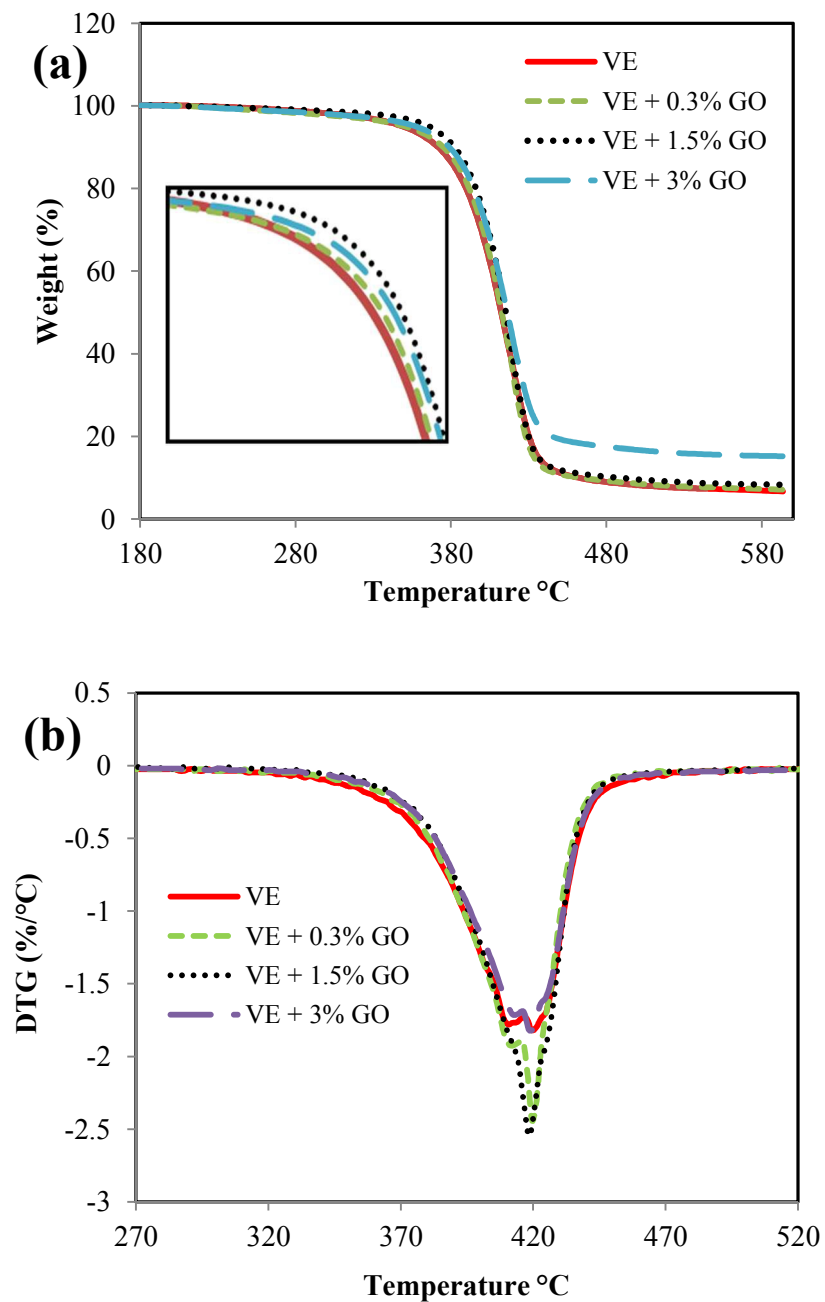
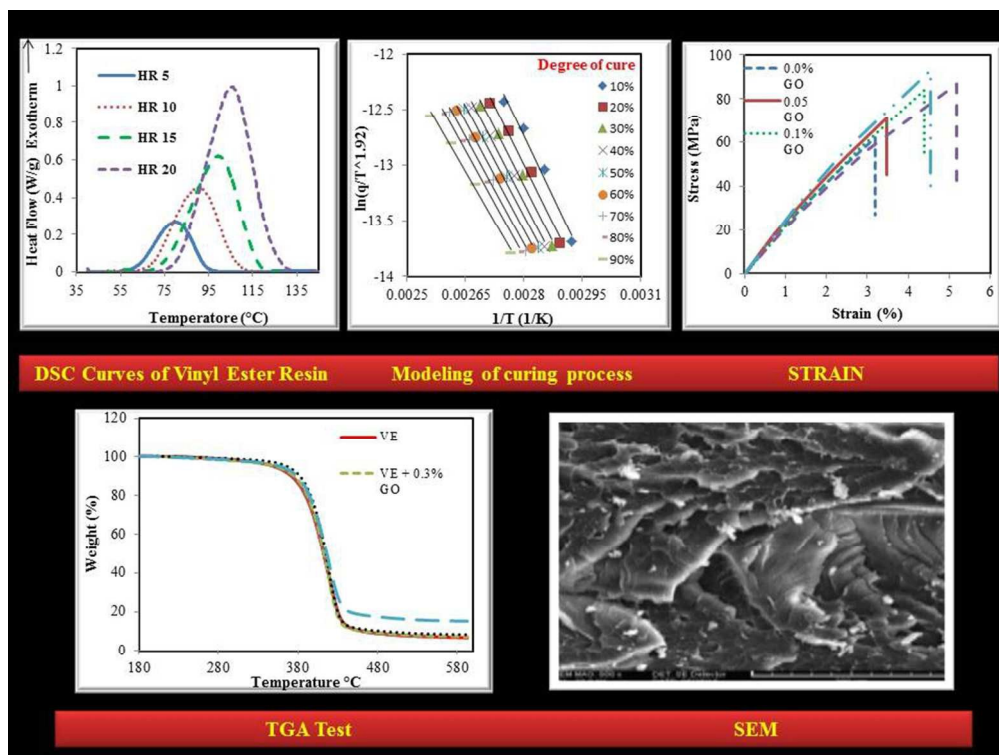


Figure 16



254x190mm (96 x 96 DPI)